

# Thermalization process of a photo-generated plasma in semiconductors

M.A. Rodríguez-Meza<sup>1,2,\*</sup> and J.L. Carrillo<sup>1</sup>

<sup>1</sup>*Instituto de Física, Universidad Autónoma de Puebla*

*Apartado postal J-48, 72570 Puebla, Pue., Mexico*

*e-mail: \*mar@sirio.ifuap.buap.mx*

<sup>2</sup>*Instituto Nacional de Investigaciones Nucleares*

*Apartado postal 18-1027, 11801 México, D.F., Mexico*

Recibido el 20 de junio de 2001; aceptado el 30 de noviembre de 2001

The kinetics of ultra-fast processes which leads to the thermalization condition of a photo-excited plasma in semiconductor systems is studied theoretically. We analyze the time evolution of a carrier population generated by a finite optical pulse, from the beginning of the pulse until the time in which the carrier population reaches a quasi-equilibrium condition. We calculate the energy fluxes caused by the main interaction mechanisms along the different stages the system passes through. Our analysis is done by using a set of non-linear rate equations which govern the time evolution of the carrier population in the energy space. We consider the main interaction mechanisms, including dynamic screening and phonon population effects.

*Keywords:* Photo-excited plasma; thermalization; ultrafast processes in semiconductors

Se estudia la cinética de los procesos ultrarrápidos que llevan a la condición de termalización de un plasma fotoexcitado en sistemas semiconductores. Analizamos la evolución temporal de una población generada por un pulso óptico finito, desde el comienzo del pulso hasta el tiempo en el que la población alcanza una condición de cuasi equilibrio. Calculamos los flujos de energía causados por los mecanismos principales de interacción a lo largo de las diferentes etapas por las que pasa el sistema. Hacemos nuestro análisis usando un conjunto no lineal de ecuaciones de razón de cambio que gobiernan la evolución temporal de la población de portadores en el espacio de energías. Consideramos los mecanismos principales de interacción, incluyendo el apantallamiento dinámico y los efectos de población de fonones.

*Descriptores:* Plasma fotoexcitado; termalización; procesos ultrarrápidos en semiconductores

PACS: 72.20.Jv; 72.20.Dp; 78.20.Bh; 78.47.+p

## 1. Introduction

The relaxation processes of photo-generated plasma systems in semiconductors exhibit two characteristic stages. The first of them, commonly called the thermalization process, is mainly governed by the rapid interactions, namely, the electron-electron ( $e-e$ ) and the electron-optical phonon interactions. In this stage the carrier distribution function (CDF) is far from equilibrium and theoretical approximations for this, based on small displacements from the equilibrium are poor approaches to describe the kinetics of these processes. This stage ends when the interaction mechanisms randomize the energy and momentum in the carrier population. This allows the CDF to reach a condition in which it is possible to define an effective temperature for the carrier system, *i.e.*, the CDF acquires a shape similar to that of an equilibrium one. The second stage of the relaxation is the so called, cooling process, and is mainly ruled by the slow interactions in the system, namely, electron-phonon ( $e-ph$ ) scattering and recombination. This process has been extensively studied since the pioneering works of the late 60's and 70's decades [1, 2]. In this stage, the time evolution of the quasi-equilibrium CDF can be described by means of simplified evolution equations for time dependent effective temperature and chemical potential [3].

There have been in the literature reported theoretical and experimental studies on the thermalization process, however

it is still not well understood [2, 4–7]. This is because the thermalization process is a stage dominated by transient effects in a far from equilibrium system. The understanding of the transient processes occurring in photo-generated carrier populations is of great relevance because it would allow a deeper physical insight on the dynamical effects of interaction mechanisms upon observable properties of the system. In addition, it could provide information, as well as a theoretical framework, to investigate some particular ultra-fast phenomena like the kinetics of thermo-transport and the kinetics of the coherent control of quantum states in mesoscopic semiconductor systems [8–10].

Thermalization depends mainly on the efficiency of the  $e-e$  scattering to redistribute the excess energy given to the system by the external sources. Once thermalized, the electronic system relaxes by dissipating the energy in excess into the lattice and by emitting radiation. Associated to each one of the stages of the relaxation process, there is a characteristic time. The first one, the thermalization time, is an effective time determined by the intrinsic characteristic times of the rapid interaction mechanisms within the system and the second one is a characteristic time determined by the interaction mechanisms of the system with the surroundings. Thermalization and cooling processes also depend on other features of the excitation, for instance the excitation time, *i.e.*, the time along which the carrier generation is produced or the time the perturbation remains switched on. The thermalization and

cooling times notoriously change if the external perturbation remains switched on over times longer than the  $e$ - $e$  collision time, or if the perturbation switching on occurs adiabatically.

We present in this paper a detailed study on the ultra-fast processes which lead to the thermalization condition in a photo-excited electron gas in polar semiconductors. We assume the semiconductor is excited by a pulsed laser. We define two quantities on which our discussion is based, namely, the thermalization time and the thermalization temperature [5]. We analyze how these quantities depend on some external variables such as the time duration of the laser pulse, the energy of excitation, the carrier concentration, and the lattice temperature.

## 2. Theory

To study the thermalization process of a photo-generated electron gas in a bulk semiconductor we use a set of rate equations we have developed to investigate several physical situations [5, 6]. These equations describe the evolution of the electron population in semiconductors under several general conditions, and consider the most important interaction mechanisms, including screening and phonon population effects. Our theoretical scheme is based in the following formalism.

Let us start by defining the carrier population in a volume element in the  $(\mathbf{r}, \mathbf{k})$ -space or  $\mu$ -space, composed of the carrier position  $\mathbf{r}$  and the carrier wavevector  $\mathbf{k}$ ,

$$\eta(\mathbf{r}, \mathbf{k}, t) = f(\mathbf{r}, \mathbf{k}, t) \frac{V}{4\pi^3} d\mathbf{r}d\mathbf{k}, \quad (1)$$

where  $f(\mathbf{r}, \mathbf{k}, t)$  is the carrier distribution function in the  $\mu$ -space and  $V$  is the crystal volume.

In a similar way, for the optical phonon population we can write

$$N_j(\mathbf{q}, t) = g_j(\mathbf{q}, t) \frac{V}{(2\pi)^3} d\mathbf{q}, \quad (2)$$

where  $j$  labels the branch,  $\mathbf{q}$  is the phonon wave vector and  $g_j(\mathbf{q}, t)$  is the phonon distribution function. In the following we will use the index  $\alpha$  to denote the couple  $(j, \mathbf{q})$ . So that  $N_\alpha$  will denote the phonon population in the mode  $\alpha$ .

An electron in a semiconductor is characterized by its position  $\mathbf{r}$ , its wavevector  $\mathbf{k}$ , and the index of the energy band. An electric field introduces a preferred direction. By assuming an homogeneous, isotropic system, and for null applied electric field, the only relevant variable is the energy, as is the case of cubic semiconductors like GaAs [6, 11]. Therefore, we can write for the carrier and phonon populations

$$\eta(\epsilon, t) = f(\epsilon, t) \frac{V dSd\epsilon}{4\pi^3 |\nabla_{\mathbf{k}} \epsilon(\mathbf{k})|}, \quad (3)$$

$$N_\alpha(t) = g_j(\mathbf{q}, t) \frac{V}{(2\pi)^3} d\mathbf{q}, \quad (4)$$

where  $dS$  is a surface element on the surface of constant energy  $\epsilon$ .

Now we wish to establish the equations which govern the time evolution of these quantities. In order to do that we assume the following. Transport and optical properties of cubic semiconductors like GaAs are explained in terms of their band structure. The band structure of a cubic-model semiconductor is composed of one conduction band with three sets of minima, and three valence bands. The minima of the conduction band are located at the  $\Gamma$  point ( $k = 0$ ), at the  $L$  points [ $\mathbf{k} = (\pi/a_0, \pi/a_0, \pi/a_0)$ ,  $a_0$  being the lattice constant], and along the  $\Delta$  lines  $\mathbf{k} = (k, 0, 0)$ . The tops of the valence bands are located at the  $\Gamma$  point. Two of them are degenerate at this point and the other is separated by spin-spin interaction. Then, we suppose a band structure composed of the valley  $\Gamma$  separated from the valley  $L$  by an energy  $\Delta$ . This model is appropriate for the description of photoexcited semiconductors where the transitions involve only the center of the Brillouin zone [11]. We assume also that the continuum of states of the valley is partitioned into a set of discrete intervals of energy  $\Delta\epsilon$ . For simplicity, and in order to have a direct reference we choose  $\Delta\epsilon$  to be the longitudinal optical (LO) phonon of energy  $\hbar\omega_{LO}$ . This choice is not an essential assumption for the development of our procedure [6].

Instead of establishing evolution equations for the quantities  $\eta(\epsilon, t)$ , we shall set up the evolution equations for these quantities integrated in the interval of range  $\Delta\epsilon = \hbar\omega_{LO}$ . So, we have

$$\eta_{\gamma i}(t) = f_\gamma(\epsilon_i, t) d_{\gamma i}, \quad (5)$$

where  $\gamma = \Gamma, L$  labels the valleys, and  $i$  the levels of energy  $\epsilon_i = i\Delta\epsilon$ ; ( $i = 0, 1, 2, \dots$ ), and

$$d_{\gamma i} = \int_{\Delta\epsilon} D_\gamma(\epsilon_i) d\epsilon = \int_{\Delta\epsilon} \frac{V dSd\epsilon}{4\pi^3 |\nabla_{\mathbf{k}} \epsilon(\mathbf{k})|} \quad (6)$$

is the number of energy states in the interval characterized by set of indexes  $(\gamma i)$ . Obviously it depends on the density of states  $D_\gamma(\epsilon)$  in the respective valley.

We obtain the evolution equation for the carrier population in the different levels in the energy space by using the conservation of the electron number, thus we can write

$$\frac{d\eta_{\gamma i}}{dt} = \sum_m (b_m - a_m) + G_{\gamma i} - R_{\gamma i}, \quad (7)$$

where  $a_m$  ( $b_m$ ) is the flux out from (into) the level  $\gamma i$  due to the interaction mechanism labeled by  $m$ . The photo-generation of carriers is accounted by  $G_{\gamma i}$ , while  $R_{\gamma i}$  denotes the recombination rate. The rate Eqs. (7) govern the evolution of the carrier system and form a set of non linear coupled differential equations where the fluxes depend on the carrier populations

$$\begin{aligned} a_m &= a_m(\eta_{\gamma i-1}, \eta_{\gamma i}, \eta_{\gamma i+1}), \\ b_m &= b_m(\eta_{\gamma i-1}, \eta_{\gamma i}, \eta_{\gamma i+1}). \end{aligned}$$

### 2.1. Scattering mechanisms

We now particularize our treatment to the case of polar semiconductors. However, the adaptation of the theory necessary

to deal with covalent semiconductors is almost direct. The evaluation of the probabilities associated to the collision mechanisms can be done by using the straightforward first-order perturbation theory. The expressions obtained by the use of the Fermi Golden rule for the transition probabilities due to the different interaction mechanisms, can be found somewhere else. The derivation of some of them and modifications of these expressions according with our theoretical framework, is almost direct, here we just discuss those details which in our opinion might need some clarification. Full details can be found in Ref. 6.

### 2.1.1. Electron-longitudinal-optical phonon interaction (polarization potential)

When a carrier undergoes an electron-logitudinal-optical phonon interaction makes a transition to the neighbour le-

vels ( $i \pm 1$ ) in the same band. Transition to different bands (inter valley) in which an optical phonon is participating is due to a different potential, the optical deformation potential [11]. For photoexcited semiconductors we are interested in the transitions occur only at the center of the Brillouin zone, and these inter valley transitions are neglected [11]. The expression for the fluxes due to the electron-logitudinal-optical phonon interaction is derived in Ref. 6 and is based on the matrix elements derived elsewhere, see for example Ref. 12.

The fluxes can be written as [6, 12, 13]

$$a = \eta_{\gamma i} \nu_{\text{op}}^{\gamma \pm}(\epsilon_i) \left( 1 - \frac{\eta_{\gamma i \mp 1}}{d_{\gamma i \mp 1}} \right), \quad (8)$$

$$b = \left( 1 - \frac{\eta_{\gamma i}}{d_{\gamma i}} \right) \nu_{\text{op}}^{\gamma \pm}(\epsilon_i) \eta_{\gamma i \pm 1}, \quad (9)$$

where

$$\nu_{\text{op}}^{\gamma \pm}(\epsilon) = \frac{\sqrt{m_{\gamma}} e^2 \hbar \omega_{\text{LO}}}{\sqrt{2} \hbar^2} \left( \frac{1}{\mathcal{E}_{\infty}} - \frac{1}{\mathcal{E}_s} \right) \left( N_{\gamma} + \frac{1}{2} \pm \frac{1}{2} \right) \frac{1}{\sqrt{\epsilon}} S_{\text{LO}}^{\gamma} \ln \left( \frac{1 + \sqrt{1 \mp \frac{\hbar \omega_{\text{LO}}}{\epsilon}}}{\pm 1 \mp \sqrt{1 \mp \frac{\hbar \omega_{\text{LO}}}{\epsilon}}} \right), \quad (10)$$

where  $\mathcal{E}_{\infty}$  and  $\mathcal{E}_s$  are the static and optical dielectric constants, respectively.  $m_{\gamma}$  is the effective mass in the  $\gamma$  valley,  $e$  is the electron charge and  $\hbar$  is the Planck constant. The upper (lower) sign is for emission (absorption). The screening effects in the  $e$ -ph interaction are included in the factor  $S_{\text{LO}}^{\gamma}$ , which in the random-phase approximation is given by [13]

$$S_{\text{LO}}^{\gamma} = \frac{N_{\gamma}}{N} \left[ 1 + \left( \frac{N_{\gamma}}{N_{\gamma}^c} \right)^2 \right]^{-1},$$

where  $N$  and  $N_{\gamma}$  are the total and  $\gamma$  valley carrier concentration respectively,  $N_{\gamma}^c$  is the threshold value for the concentration in the  $\gamma$  valley at which the screening becomes important. This critical value for the carrier concentration is given by

$$N_{\gamma}^c = \frac{\mathcal{E}_{\infty} m_{\gamma} (\hbar \omega_{\text{LO}})^3}{3^{3/2} 8 \pi e^2 \hbar^2 k_{\text{B}} T_e},$$

where  $T_e$  is the electronic temperature and  $k_{\text{B}}$  is the Boltzmann's constant.

### 2.1.2. Electron-electron interaction

The electron-electron interaction gives the nonlinear character of the Eqs. (7) and is one of the most difficult interactions to take into account. We adopt the Debye-Hückel screened potential to describe the  $e$ - $e$  interaction. We see that the scattering processes in which the magnitude of exchanged momentum is small are the most likely, because the probability diminishes as  $q^{-4}$ . Also, on the average, an electron in the valley  $\Gamma$  exchanges approximately  $\hbar \omega_{\text{LO}}$  of energy [6]. Therefore, in our energy levels scheme, carriers make transitions to the neighbour levels  $i \pm 1$  in the same band due to the  $e$ - $e$  scattering. For more details see Refs. 6 and 14.

The fluxes are given by [6]

$$a = \eta_{\gamma i} Z^{\gamma} \left[ \left( 1 - \frac{\eta_{\gamma i-1}}{d_{\gamma i-1}} \right) \sum_{\gamma' i'} \eta_{\gamma' i'} \left( 1 - \frac{\eta_{\gamma' i'+1}}{d_{\gamma' i'+1}} \right) + \left( 1 - \frac{\eta_{\gamma i+1}}{d_{\gamma i+1}} \right) \sum_{\gamma' i'} \eta_{\gamma' i'} \left( 1 - \frac{\eta_{\gamma' i'-1}}{d_{\gamma' i'-1}} \right) \right], \quad (11)$$

$$b = \left( 1 - \frac{\eta_{\gamma i}}{d_{\gamma i}} \right) Z^{\gamma} \left[ \eta_{\gamma i+1} \sum_{\gamma' i'} \eta_{\gamma' i'} \left( 1 - \frac{\eta_{\gamma' i'+1}}{d_{\gamma' i'+1}} \right) + \eta_{\gamma i-1} \sum_{\gamma' i'} \eta_{\gamma' i'} \left( 1 - \frac{\eta_{\gamma' i'-1}}{d_{\gamma' i'-1}} \right) \right], \quad (12)$$

where Pauli exclusion principle has been taken into account and

$$Z^{\gamma} = \frac{e^2 \sqrt{\pi m_{\gamma} k_{\text{B}} T_e}}{2^2 \hbar^2 \mathcal{E}_{\infty} N} \frac{1}{1 + \frac{N}{N_{\text{ee}}^{\gamma}}}. \quad (13)$$

The square brackets factor takes into account the screening effects. These become important when the carrier concentration  $N$  reaches a critical value  $N_{ee}^\gamma$  given by

$$N_{ee}^\gamma = \frac{4m_\gamma \mathcal{E}_\infty (k_B T_e)^2}{\pi^2 \hbar^2 e^2}.$$

The expression for the total probability, Eq. (13), is an heuristic useful expression, that allows us to determine in an easy way the ranges of carrier concentration and electronic temperature, in which the energy exchange through  $e$ - $e$  scattering is the dominant mechanism in the kinetics of the system.

## 2.2. Generation and recombination

The dynamics of carriers under intense laser irradiation has been described by Ferry [15]. Here we adopt the following procedure to describe the generation and recombination processes. The rate equation which governs the effect of the generation and recombination processes on the CDF can be written as

$$\frac{d\eta_{\Gamma i}}{dt} = G_{\Gamma i} - R_{\Gamma i} \quad (14)$$

the first RHS term represents the photo-generation of carriers and the second one represents the recombination processes. In direct gap semiconductors the photo-excitation involves the top of the valence band and the bottom of the conduction band which are at the  $\Gamma$  point. For indirect gap semiconductors it is necessary the participation of a phonon in order to conserve momentum. In this report we are interested in direct gap semiconductors, therefore, we shall assume only generation of carriers to the  $\Gamma$  valley, therefore, the generation term can be written as [6]

$$G_{\Gamma i} = G_p(t) \delta_{i,i_p} \left(1 - \frac{\eta_{\Gamma i}}{d_{\Gamma i}}\right) \left(1 - \sigma \frac{\eta_{\Gamma i}}{d_{\Gamma i}}\right), \quad (15)$$

where  $i_p \Delta \epsilon$  is the excitation energy (measured from the bottom of the conduction band).  $G_p(t)$  is proportional to the rate of generation, *i.e.*, the number of excited carriers per unit time given by

$$G_p(t) = G_p^* G(t) = \frac{P_L}{A d \hbar \omega_L} G(t),$$

where  $P_L$  is the laser power,  $\hbar \omega_L$  is the photon energy,  $d$  is the penetration length, and  $A$  is the area of illumination. The dimensionless function  $G(t)$  is conveniently chosen in order to model a given experimental condition. For instance, for the case of a steady state  $G(t) = 1$ . The factor  $\sigma$  is given by  $\bar{f}/f$ , where  $\bar{f}$  is the hole distribution, and in general is a function which depends upon  $\epsilon$  and  $t$ . In steady state processes  $\sigma$  accounts for the degree of compensation in the material.

The rate of recombination can be expressed as  $R = R^R + R^N$ , *i.e.*, it is the addition of the radiative and non radiative components of the recombination.

In this work we assume  $R_{\Gamma i} = w \eta_{\Gamma i}$  where  $w$  is defined as

$$w = \left\langle \frac{1}{\tau_{\text{rec}}} \right\rangle = \frac{\int \frac{1}{\tau_{\text{rec}}} f(\epsilon) \sqrt{\epsilon} d\epsilon}{\int f(\epsilon) \sqrt{\epsilon} d\epsilon}, \quad (16)$$

and  $\tau_{\text{rec}}$  has to be calculated for the pertinent kind of recombination.

## 2.3. Phonon population effects

We have mentioned that a high population of phonons can produce some important effects and these effects are more notorious in the case of the LO phonons [16]. However, the number of LO modes is limited by the magnitude of the electron wave vector. These limits can be easily obtained by applying the energy and momentum conservation conditions to a transition in which an electron with an energy near the maximum energy  $\epsilon_{\text{max}}$  absorbs a LO phonon. In this way one obtains

$$q_{\text{min}} = \frac{\sqrt{2m_\gamma \epsilon_{\text{max}}}}{\hbar} \left[ \sqrt{1 + \frac{\hbar \omega_{\text{LO}}}{\epsilon_{\text{max}}}} - 1 \right],$$

and

$$q_{\text{max}} = \frac{\sqrt{2m_\gamma \epsilon_{\text{max}}}}{\hbar} \left[ \sqrt{1 + \frac{\hbar \omega_{\text{LO}}}{\epsilon_{\text{max}}}} + 1 \right].$$

Of course in this energy scheme it is not possible to know the wave vector of the absorbed phonon. In order to describe phonon population effects we need to link the carrier system to the phonon population. To this end we use the following evolution equation for the whole phonon population  $N_{\text{LO}}$

$$\frac{dN_{\text{LO}}}{dt} = \frac{1}{U} \sum_{\gamma i} \eta_{\gamma i} \left[ \nu_{\text{op}}^{\gamma+}(\epsilon_i) \left(1 - \frac{\eta_{\gamma i-1}}{d_{\gamma i-1}}\right) - \nu_{\text{op}}^{\gamma-}(\epsilon_i) \left(1 - \frac{\eta_{\gamma i+1}}{d_{\gamma i+1}}\right) \right] - \frac{N_{\text{LO}} - N_{\text{LO}}^{\text{eq}}}{\tau_{\text{LO}}}, \quad (17)$$

where  $U$  is the number of permitted modes per unit volume,

$$U = \int_{q_{\text{min}}}^{q_{\text{max}}} \frac{dq}{(2\pi)^3},$$

and  $N_{\text{LO}}^{\text{eq}}$  is the equilibrium total LO phonon population and  $\tau_{\text{LO}}$  is its time life.

The set of Eqs. (7) and (17) with the respective expressions for the fluxes are the basis of this model. These equations can be easily extended to represent a more general situation. For instance, the hypothesis of parabolic valleys can be changed to

allow the description with a more realistic band structure. The solution to these rate equations can be considerably simplified by the use of effective collision frequencies (ECF). These frequencies are the average over the band of the scattering frequencies defined for each of the energy levels and which are the factors appearing in the fluxes. We would like to notice here that the information about the band structure and other symmetries of the system is contained in the ECFs. Thus, this approach can be used to study ultra-fast phenomena in quantum wells, superlattices and heterostructures, as well as bulk semiconductors systems [6, 17].

### 3. Normalized rate equations

For not very high carrier concentration we can neglect the inter valley transitions. The threshold in which we can neglect inter valley transitions depends on the material, for GaAs this threshold is  $1 \times 10^{18} \text{ cm}^{-3}$  [11]. If additionally one assumes a non-degenerate electron gas and use the ECFs as defined before, the rate equations (7) and (17) become notoriously simplified. The use of the ECFs in our description is in fact justified by the smooth behavior of the scattering probabilities as function of the energy. Hence, under these conditions the rate equations can be cast into

$$\begin{aligned} \frac{d\chi_i}{dt} = & \nu_o^+(\chi_{i+1} - \chi_i) + \nu_o^-(\chi_{i-1} - \chi_i) \\ & + ZN_{\max}\chi(\chi_{i+1} - 2\chi_i + \chi_{i-1}) \\ & + ZN_{\max}\chi_0(\chi_i - \chi_{i-1}) + g_p\delta_{0,i_p} - w\chi_i, \end{aligned} \quad (18)$$

for  $i \neq 0$  and for  $i = 0$  we have

$$\begin{aligned} \frac{d\chi_0}{dt} = & \nu_o^+\chi_1 - \nu_o^-\chi_0 + ZN_{\max}\chi(\chi_1 - \chi_0) \\ & + ZN_{\max}\chi_0\chi_0 + g_p\delta_{0,i_p} - w\chi_0. \end{aligned} \quad (19)$$

For the phonon population in excess,  $N_{\text{LO}}^{\text{exc}} = N_{\text{LO}} - N_{\text{LO}}^{\text{eq}}$ , we have

$$\frac{dN_{\text{LO}}^{\text{exc}}}{dt} = \frac{1}{u} [\nu_o^+(\chi - \chi_0) - \nu_o^-\chi] - \xi N_{\text{LO}}^{\text{exc}}, \quad (20)$$

where the populations have been normalized to the maximum reachable carrier concentration  $N_{\max}$ , *i.e.*,  $\chi_i = \eta_i/N_{\max}$ ;  $\chi = \sum_i \chi_i$ ;  $u = U/N_{\max}$ ; and  $g_p = G_p/N_{\max}$ . The ECF  $\nu_o^\pm$  has just the dominant term of the  $e$ -LO phonon interaction, and  $\xi = 1/\tau_{\text{LO}}$ . Notice the differences between the rate equation for  $i = 0$  and  $i \neq 0$ .

### 4. Results and discussion

For the sake of brevity, from here on, we will refer as carrier distribution function to the set of values  $\{\chi_i\}$  of the carrier population at the different energy intervals on the conduction band. The link of this distribution with the actual out of equilibrium CDF is given by the expression (5). We start our discussion by defining two physical quantities inherent to

the time evolution of the photo-generated carrier population. More specifically, we wish to characterize by means of these physical quantities, the stage in which the system reaches the thermalization condition. These quantities are the thermalization time  $t^*$  and the thermalization temperature  $T_e^*$  [5]. Our definition of these quantities intend to be phenomenologically amenable. Thus,  $t^*$  is defined as the time interval, measured from the beginning of the laser pulse, that the carrier system requires to reach a distribution shape which can be fitted by means of a single exponential function,

$$\chi_i = A \exp\left(-i \frac{\Delta\epsilon}{k_B T_e^*}\right). \quad (21)$$

Here  $A$  is a normalization constant. The quantity  $T_e^*$ , which makes the fitting possible, defines the thermalization temperature. This last definition closely resembles the way in which the carrier temperature of a hot electron system is experimentally determined [1]. We proceed by numerically integrating Eqs. (18), (19), and (20) under different physical conditions and seeking the effects of the external variables on  $t^*$  and  $T_e^*$ . Starting at the pulse beginning, the carrier population generated in the conduction band evolves due to the collision mechanisms according to the rate Eqs. (18), (19), and (20). At each step of the numerical integration we are able to calculate the CDF and the corresponding values of the ECFs. In the initial steps of the numerical integration, in general the CDF differs clearly of the shape of a thermalized distribution, *i.e.*, a Boltzmann factor. Within subsequent iterations the CDF gradually adopts a decreasing shape, which eventually, at  $t = t^*$ , admits a fitting by means of a simple decreasing exponential function. The exponent in that event is inversely proportional to  $T_e^*$  [1, 2, 5, 6]. This is the way in which we proceed to evaluate  $t^*$  and  $T_e^*$ .

In order to make concrete calculations we consider the well known values of the electronic band structure, phonon dispersion relations and material parameters of GaAs. For example,  $\hbar\omega_{\text{LO}} = 36 \text{ meV}$  and the energy extent of the conduction band at the  $\Gamma$  point is 1 eV. This means that the necessary number of energy levels is 28. Other GaAs material parameters can be found Refs. 6 and 11, and references there in. At  $t = 0$  in an empty conduction band a laser pulse of duration  $t_p$  injects  $g_p$  electrons per unit time with an energy  $i_p$  in units of  $\Delta\epsilon$  and above of the bottom of the band.

Before starting our analysis of the thermalization process we discuss briefly the physical suitability of our carrier temperature definition. By means of expression (21) we have defined at time  $t^*$  the thermalization temperature  $T_e^*$ . At subsequent times one also might use this procedure to calculate the carrier temperature  $T_e(t)$ . We have studied the time evolution of this quantity under various different physical conditions. Our results show a good agreement with experimental data [6]. Firstly we analyze the effect of the pulse duration on the time evolution of the carrier temperature  $T_e$ , as well as on the main interaction frequencies, *i.e.*,  $e$ - $e$ ,  $e$ -ph emission, and  $e$ -ph absorption;  $z$ ,  $\nu^+$ , and  $\nu^-$  respectively. In Fig. 1 (upper) we show  $T_e(t)$  for an instantaneous pulse  $t_p = 0 \text{ ps}$

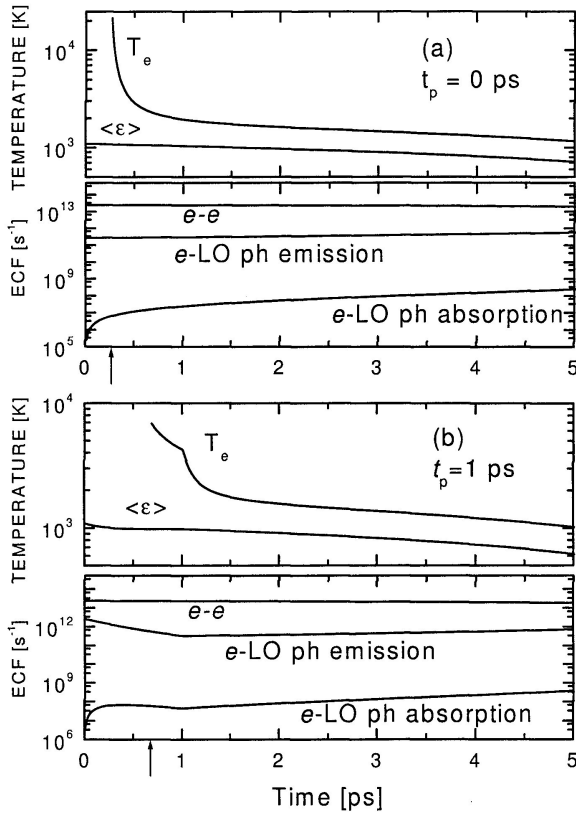


FIGURE 1. Time evolution of the effective carrier temperature  $T_e$  and the kinetic temperature obtained from the mean energy in units of  $K$ ,  $2\langle\epsilon\rangle/3k_B$ . The time evolution of the main ECFs are shown in the lower part. The pulse duration is for upper figure  $t_p = 0$  ps and for lower figure  $t_p = 1$  ps.

which excites  $N = 10^{17} \text{ cm}^{-3}$  electrons at an energy level  $i_p = 4$ . We have also plotted the behavior of the kinetic temperature defined by  $2\langle\epsilon\rangle/3k_B$ . We show the behavior of these quantities since the pulse starts, until times well above the thermalization condition is reached. We assume in this calculation a lattice temperature  $T_L = 10$  K and take from the literature a commonly used value of the damping constant for the LO-phonons  $\tau_{LO} = 12$  ps. Notice that the resulting thermalization time is  $t^* = 0.26$  ps (indicated by an arrow in the Figure). In the lower part of Fig. 1 (upper figure) appears the time evolution of the main ECFs during this relaxation process. In Fig. 1 (lower) we show these quantities for a pulse of finite duration  $t_p = 1$  ps. In this case we obtain  $t^* = 0.65$  ps (also indicated by an arrow in the Figure). From the comparison of these Figures we may conclude that the pulse duration has a clear influence on the general characteristics of these quantities, namely, the pulse duration modifies  $t^*$  and  $T_e^*$ . Thus, this is one of the external variables which determines the interaction mechanisms and their relative importance in the thermalization process of the CDF. The evolution of the main ECFs provide detailed information, at every stage of the relaxation process, about the relative incidence of the main collision mechanisms in the kinetics of the carrier system. We wish to recall here that we are considering

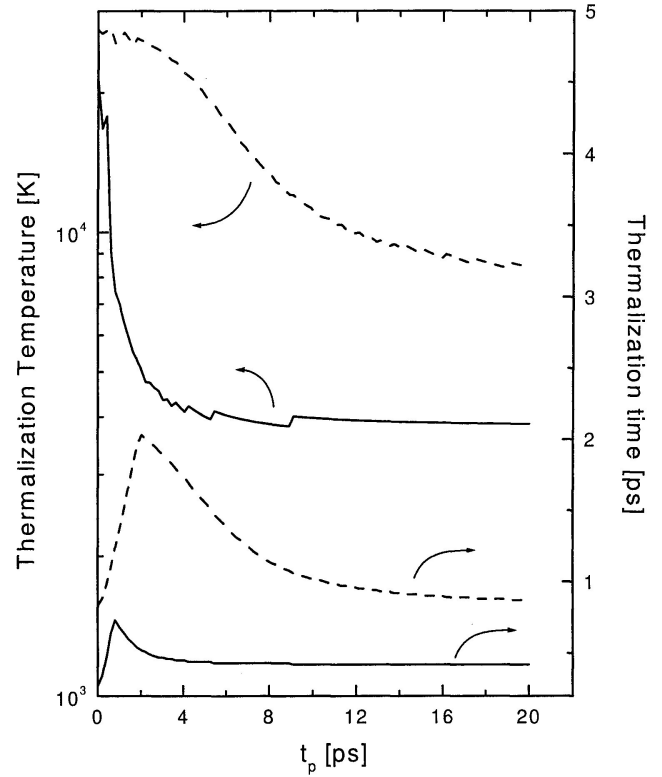


FIGURE 2. Temperature and time of thermalization vs. pulse duration for two values of the excitation energy level. (—) correspond to  $i_p = 4$  and (---) corresponds to  $i_p = 10$ . The carrier concentration is  $N = 10^{17} \text{ cm}^{-3}$ . The scale for  $t^*$  is at the right axis of the graph.

in our treatment screening and phonon population effects. We notice that the  $e-e$  ECF varies rather slightly along the period of time considered, but the ECFs corresponding to  $e-ph$  interaction exhibit more pronounced variations. Notice the semi-logarithmic scale of the graphics. In Fig. 1 (lower) one can observe a clear abrupt change in the time evolution of the electronic temperature at the time when the pulse ends. We now restrict our analysis to the thermalization process and, on the basis of the behavior of the ECFs in this stage, we discuss the effect of  $t_p$  and other external parameters on  $T_e^*$  and  $t^*$ .

Figure 2 shows the changes which the pulse duration induces on  $T_e^*$  and  $t^*$ . We consider here a carrier population  $N = 10^{17} \text{ cm}^{-3}$ , a lattice temperature  $T_L = 10$  K, and two energy levels of excitation  $i_p = 4$  and  $i_p = 10$ . Notice that the scale for  $t^*$  appears on the right hand side of the graphs. We observe that both  $T_e^*$  and  $t^*$  reach higher values for  $i_p = 10$  than they do for  $i_p = 4$ , this is so all along the interval of  $t_p$ . This result is easily explained if we realize that for  $i_p = 10$  the carrier system receives a higher excess energy than it does for  $i_p = 4$ , it leads the carrier system to reach, comparatively, a higher value of  $T_e^*$  and due to the also relatively larger number of energy states accesible to the carriers, the thermalization condition requires a longer time. The other aspect of the Figures worthy of mention is the differen-

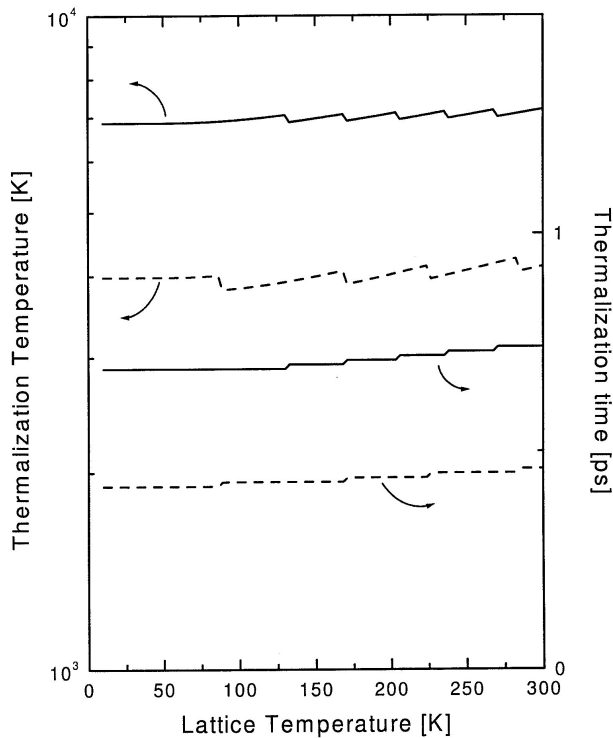


FIGURE 3.  $T_e^*$  and  $t^*$  as a function of the lattice temperature  $T_L$  for  $N = 10^{17} \text{ cm}^{-3}$  and two pulse durations  $t_p = 1 \text{ ps}$  (—) and  $t_p = 10 \text{ ps}$  (- - -).

ce between the behavior of  $T_e^*$  and  $t^*$  in the region of low values of  $t_p$ , for both  $i_p = 4$  and  $i_p = 10$ . While  $t^*$  increases with  $t_p$  to reach a maximum value and then decreases,  $T_e^*$  decreases monotonously. This last asymptotic behavior would correspond to the values of time and temperature of thermalization that the system would reach in the event of a CW laser mode experiment in which the same rate of generation is kept during a long time, *i.e.*,  $t_p \rightarrow \infty$ . Again here the larger energy in excess received by the carriers and the large energy of states of the system with  $i_p = 10$  explain the corresponding larger value of  $T_e^*$  and  $t^*$ , in comparison to the respective results for  $i_p = 4$ .

The carrier population at the lowest level in the conduction band governed by Eq. (19) has an important role in the thermalization process [14]. The shoulder shown in the behavior of  $t^*$  as a function of the pulse duration  $t_p$ , is caused predominantly by two aspects of the carrier kinetics. One of them is the time necessary to form, in the lowest level, a carrier population, which in the thermalized condition must exponentially decay for increasing energies. The other aspect is the rate of carrier generation at the level of energy  $i_p$ , which in the thermalized condition should be small enough in order that this generation at each step becomes included in the error tolerance in the fitting.

Figure 3 shows how the values of  $t^*$  and  $T_e^*$  change with the lattice temperature  $T_L$ . We consider here two different pulse durations  $t_p = 1 \text{ ps}$  (continuous line) and  $t_p = 10 \text{ ps}$  (dashed line), an excitation energy  $i_p = 4$  and a carrier con-

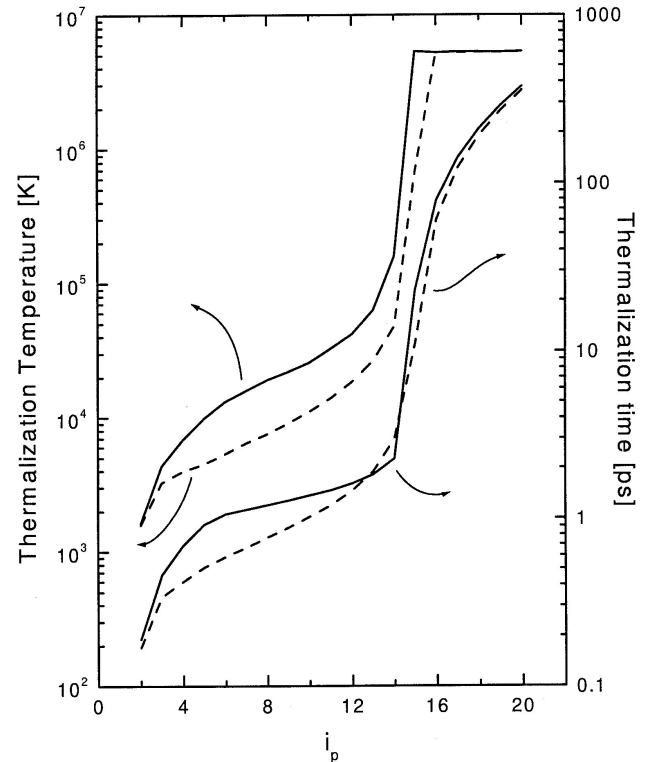


FIGURE 4.  $T_e^*$  and  $t^*$  vs. energy level of excitation  $i_p$  for the same pulses as in Fig. 3.

centration  $N = 10^{17} \text{ cm}^{-3}$ . We observe that the lattice temperature has a rather mild effect on the thermalization process. According to the behavior of the ECFs during the thermalization process (Fig. 1), the major influence must come from phonon absorption events, whose contribution is larger for higher  $T_L$  values, this is so, because it propitiates a high LO-phonon population in such a way that, comparatively to the phonon emission, phonon absorption increases its participation in the kinetics of the carrier system.

In Fig. 4, for the same pulses as in Fig. 3, we have depicted our results for  $t^*$  and  $T_e^*$  as a function of the energy of excitation  $i_p$ . The dashed curves correspond to  $t_p = 10 \text{ ps}$ . The non-linear nature of the  $e-e$  interaction is revealed in these results. We observe that a general behavior of both quantities is that, they increase with increasing values of the excitation energy, however, this behavior is non-monotonic. The dependence of the carrier temperature upon the carrier concentration and upon the energy of excitation have been studied since the 70's decade. We have studied this dependences theoretically. In particular we have found that strong changes in the CDF, associated with the non-linear nature of the  $e-e$  interaction, can be induced by varying the excitation energy [18]. The abrupt change in  $T_e^*$  and  $t^*$  about  $i_p = 14$  is a manifestation of this sensitive dependence. There has been in the literature some discussion regarding to this point. In particular, this phenomenon has been analyzed as a phase transition like behavior of the carrier population in the lowest level of energy [14].

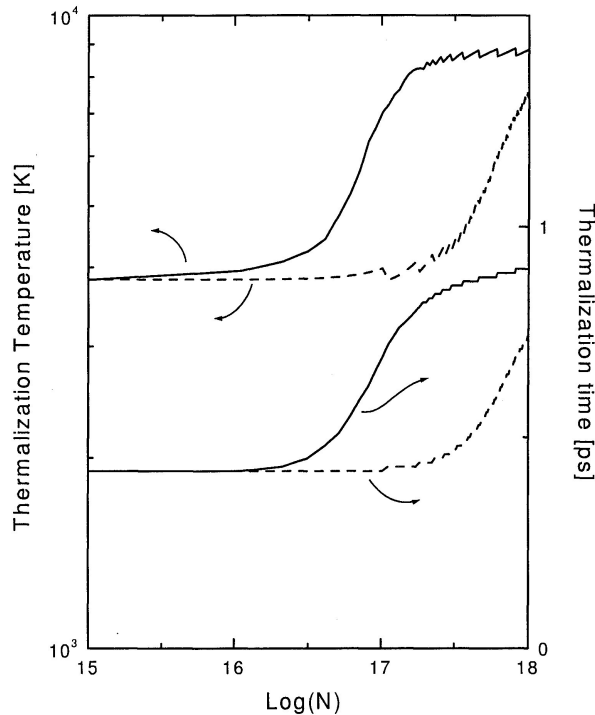


FIGURE 5. Dependence of  $T_e^*$  and  $t^*$  on the carrier concentration. Energy of excitation  $i_p = 4$  and pulses of  $t_p = 1$  ps (—) and  $t_p = 10$  ps (---).

In Fig. 5 we show the dependence of  $T_e^*$  and  $t^*$  on the carrier concentration. We also consider here two pulses of duration  $t_p = 1$  ps, continuous lines, and  $t_p = 10$  ps, dashed lines, an energy level of excitation  $i_p = 4$ , and a lattice temperature  $T_L = 10$  K. The non-linear dependence of  $t^*$  and  $T_e^*$  upon the carrier concentration is clearly exhibited. Notice that for carrier concentrations larger than  $10^{17}$  cm $^{-3}$  the screening effects begin to be noticeable. Screening turns the  $e$ - $e$  interaction less effective in thermalizing the CDF and reduces the rate at which  $e$ -ph scattering takes out energy from the electronic system, in this way, both  $T_e^*$  and  $t^*$  increase with the carrier concentration.

## 5. Comments and remarks

The criterion we have applied here to define  $T_e^*$  and  $t^*$  by means of the expression (21) may require some improvement.

We think that the least squares fitting to an exponential function, although it resembles an experimental procedure, the included inherent error could be the origin of some of the uneven behavior we observe in various of our results. However, the agreement of our results in the description of the cooling and the steady state processes in hot electron systems [6], with the experimental data, provides support to our theoretical model to describe the ultra-fast phenomena which lead a photo-generated carrier population to reach the thermalized condition. The reported experimental and theoretical results on the subject of the kinetics of the thermalization [2] also support our definition. One of the advantages of our “kinetic” approach is that, due to the fact that ECFs depend only on the band structure of the system and consequently on the system dimensionality, it can be applied to study some ultra-fast phenomena in systems of reduced dimensionality and also systems with a small number of particles. In fact we have applied these theoretical framework to study some transport phenomena in mesoscopic semiconductor heterostructures [17]. An additional interesting characteristic of this theoretical procedure is that, the required numerical calculations are not at all expensive. All the results we present in this paper can be obtained in a few minutes in an ordinary PC. In our analysis we have focused our attention to the role that the main interaction mechanisms play, however, the inclusion of some other scattering processes in the kinetics of the system is a simple task in this theoretical scheme [6].

In conclusion, we have presented a detailed analysis of the thermalization process in terms of the relevant external parameters, *i.e.*, laser pulse duration, energy of the photoexcitation, intensity of the photoexcitation, and lattice temperature. We defined two physical parameters inherent to the time evolution of the system on which the analysis of thermalization have been done, the thermalization time and temperature. We have found that the lattice temperature has a negligible influence on  $T_e^*$  and  $t^*$ . The other three external parameters clearly influence the thermalization process.

## Acknowledgements

The partial financial support by CONACyT (México) is acknowledged.

1. J. Shah and R.C.C. Leite, *Phys. Rev. Lett.* **22** (1969) 1304; J. Shah, *Phys. Rev. B* **10** (1974) 3697; J. Shah, *Solid State Electron.* **21** (1978) 43.
2. *Hot Carriers in Semiconductors*, edited by K. Hess, J.-P. Leburton, and U. Ravaioli, (Plenum Press, New York, 1996); *Hot Carriers in Semiconductor Nanostructures*, edited by J. Shah, (Academic Press, San Diego, CA, 1992).
3. See for instance: R. Luzzi and A.R. Vasconcellos, in *Semiconductors Probed by Ultrafast Laser Spectroscopy*, edited by R.R. Alfano, (Academic Press, Orland, FL, 1984), Vol. 1, p. 135; A.C.S. Algarte and R. Luzzi, *Phys. Rev. B* **27** (1983) 7563.
4. E. Heiner, *Phys. Stat. Sol. B* **144** (1987) 653.
5. M.A. Rodríguez, J.L. Carrillo, and J. Reyes, *Phys. Rev. B* **35** (1987) 6318; M.A. Rodríguez, J.L. Carrillo, and J. Reyes, *Solid State Commun.* **53** (1985) 789.



6. J.L. Carrillo and M.A. Rodríguez, *Phys. Rev. B* **44** (1991) 2934; M.A. Rodríguez, Ph.D. Thesis, Universidad Autónoma de Puebla (1988), unpublished.
7. K.W. Sun, M.G. Kane, and S.A. Lyon, *Europhys. Lett.* **26** (1994) 123; M.G. Kane, K.W. Sun, and S.A. Lyon, *Phys. Rev. B* **50** (1994) 7428.
8. See for instance the *Phys. Stat. Sol. B* (2000), issue devoted to the proceedings of the SLAFES-XV, Cartagena, Colombia (1999).
9. X. Hu and W. Potz, *Phys. Rev. Lett.* **82** (1999) 3116.
10. M.U. Wehner, M.H. Ulm, D.S. Chemla, and M. Wegener, *Phys. Rev. Lett.* **80** (1998) 1992.
11. J. Shah, *Ultrafast Spectroscopy of Semiconductors and Semiconductor Nanostructures*, 2nd edition, *Springer Ser. Solid-State Sc.*, (Springer-Verlag, Berlin Heidelberg, 1999), Vol. 115.
12. E.M. Conwell, *High Field Transport in Semiconductors*, edited by F. Seitz, D. Turnbull and H. Ehrenreich, (Academic Press, New York, 1967), Suppl. 9.
13. E.J. Yoffa, *Phys. Rev. B* **23** (1981) 1909.
14. M.A. Rodríguez-Meza, *Phys. Rev. B* **64** (2001) 233320.
15. D.K. Ferry, *Phys. Rev. B* **18** (1978) 7033.
16. W. Potz and P. Kocevar, *Phys. Rev. B* **28** (1983) 7040.
17. L. Meza-Montes, J.L. Carrillo, and M.A. Rodríguez, *Physica B* **225** (1996) 76; L. Meza-Montes, J.L. Carrillo, and M.A. Rodríguez, *ibid.* **228** (1996) 279.
18. J.L. Carrillo and J. Reyes, *Phys. Rev. B* **29** (1984) 3172.